M. BIGAJ*,#, S. BOCZKAL*, J. ŻELECHOWSKI*, M. GAWLIK*, M. MITKA*

# HEAT TREATED AZ61 MAGNESIUM ALLOY OBTAINED BY DIRECT EXTRUSION AND CONTINUOUS ROTARY EXTRUSION PROCESS

The results of studies carried out on the heat treated AZ61 magnesium alloy extruded by two methods, i.e. direct extrusion and continuous rotary extrusion, were presented. As part of the work, parameters of the T6 heat treatment were proposed and aging curves were plotted. The solution heat treatment process was accompanied by the grain growth. During artificial aging, due to the decomposition of solid solution, the β-$Mg_{17}Al_{12}$ phase was precipitated from the supersaturated α solution. It precipitated in a coagulated form at the grain boundaries and in the form of fine-dispersed plates arranged in a preferred direction relative to the grain orientation. Rods obtained by continuous rotary extrusion, unlike those made by the direct process, exhibited a low degree of texturing and lack of anisotropic properties.

*Keywords*: AZ61, heat treatment, $Mg_{17}Al_{12}$, continuous rotary extrusion, direct extrusion

## 1. Introduction

The consumption of magnesium alloys has considerably grown in recent years. This trend is progressing because of the pressure to reduce $CO_2$ emissions, and is particularly evident in the automotive industry, where it manifests itself in an attempt to reduce the weight of vehicles. Magnesium is 36% lighter than aluminum and 78% lighter than iron. Magnesium alloys used most commonly in the automotive industry are those included the Mg-Al system. Magnesium alloy components are produced by various processes, like casting, extrusion, rolling or forging. The most important methods increasing the alloy resistance to plastic deformation include grain refinement, solution hardening, precipitation hardening and cold plastic working. Many of the currently used high-strength alloys are manufactured by one or many of these processes [1].

In Mg-Zn and Mg-RE alloys, the precipitation hardening proceeds in the same way as in aluminum alloys, since the arising GP zones are gradually transformed into phases coherent first and non-coherent next with the alloy matrix. In Mg-Al alloys (including Mg-Al-Zn), the GP zones are not formed, and from the supersaturated solid solution, the $Mg_{17}Al_{12}$ phases are precipitated. The precipitation occurs in a wide range of temperatures, assuming two different morphologies: the discontinuous precipitation having an origin at the grain boundaries and continuous precipitation in the grain interior. Continuous precipitation involves the nucleation of an $Mg_{17}Al_{12}$ phase coherent with matrix (without the formation of GP zones), combined with progressive growth of particles during aging. On the other hand, discontinuous precipitation consists in the decomposition of solid solution and formation of a layered structure. The layers are composed of alternately arranged plates of the $Mg_{17}Al_{12}$ phase non-coherent with matrix and the solid solution of aluminum in magnesium with aluminum content close to equilibrium. The discontinuous transformation starts at the grain boundaries of the supersaturated solid solution. The diffusion of atoms during transformation forms colonies of plates growing inside the grains. Aging of AZ alloys promotes the formation of precipitates of the $Mg_{17}Al_{12}$ phase located at grain boundaries, of discontinuous precipitates in the form of alternately arranged plates of the α and β solutions, and of continuous precipitates forming fine plates of the β phase. Continuous precipitation is characterized by the directional arrangement of plates, dependent on the crystallographic orientation of individual grains. Most of the forming precipitates are parallel to the base $[11\overline{2}0]$ direction. The predominant Burgers relationships of crystallographic orientations between the β phases and the matrix are $(011)_p$ // $(0001)_m$ planes and $[1\overline{1}1]_p$ // $[2\overline{1}\overline{1}0]_m$ directions. The particles of continuous precipitates act as efficient obstacles to the moving dislocations when, due to their orientation, they intersect the slip plane [2, 3, 4].

In previous studies, conducted at the Institute, magnesium alloys AZ80A and ZK60A after plastic processing and heat treatment were examined [5-6]. The aim of this study is to examine the precipitation processes occurring during heat treatment of the rods of AZ61 alloy produced by the methods of direct extrusion and continuous rotary extrusion.

## 2. Material and methods

Studies were carried out on samples taken from the AZ61 alloy rods processed by the direct extrusion and Continuous Rotary Extrusion (CRE) in F condition, subjected next to the solution heat treatment and aging. The feedstock for CRE was composed of 10 mm diameter rods made by the direct extrusion. The profiles extruded by CRE were ϕ9 mm rods.

*  INSTITUTE OF NON-FERROUS METALS IN GLIWICE, LIGHT METALS DIVISION, 16 PIŁSUDSKIEGO STR., 32-050 SKAWINA, POLAND

#  Corresponding author: mbigaj@imn.skawina.pl

The examined profiles were extruded in a horizontal direct-indirect extrusion 500T capacity press and in a Conform MC-260 device for the continuous rotary extrusion. The equipment is available at the Institute of Non-Ferrous Metals in Gliwice Light Metals Division Skawina.

Table 1 shows the designation of samples and the results of chemical analysis made with an ARL 4460 Optical Emission Spectrometer from Thermo Scientific.

Two-step heat treatment of the test material consisted in solutionizing, i.e. annealing at 400 °C for 3 hours with cooling in water, and artificial aging at 180 °C for 1, 6, 12, 24, 28, 96, 192, 240 and 312 hours.

Aging curves were plotted based on Brinell hardness measurements taken with a Duramin 2500E hardness tester. Microstructure with the revealed grains was examined in polarized light using an OLYMPUS GX71 light microscope. Studies of the precipitation process were carried out by scanning electron microscopy (SEM) with chemical analysis in microregions (EDS) using an Inspect F50 microscope from FEI and a Tecnai G2 20 TEM microscope. Texture of the test material was examined by X-ray diffraction on a Bruker D8 Advance apparatus. The reverse pole figures are the result of transformations of the X-ray diffraction intensities obtained in the cross-sections of the examined magnesium rods.

## 3. Results and discussion

In the first stage of studies, to determine the effect of heat treatment, tests covered the as-extruded base material (F condition), processed next by the direct extrusion or CRE. The structure of the AZ61-P alloy was characterized by the presence of very fine grains of the 5.5 µm size (Fig. 1a, Table 2). EDS analysis combined with SEM (Fig. 1b) has revealed the presence of the two types of precipitates: Mg-Al phase additionally containing Si and Zn, and precipitates of the Al-Mn-Si type. Hardness of the alloy processed by direct extrusion was higher than the hardness of the material extruded by CRE (71.3 HB and 69 HB, respectively).

The AZ61-CRE alloy in F condition had slightly larger grains with an average of 7.7 µm (Fig. 2a, Table 2). As revealed by TEM, the size of the Mg-Al phase precipitates has never exceeded the value of approx. 2 µm (Fig. 2c).
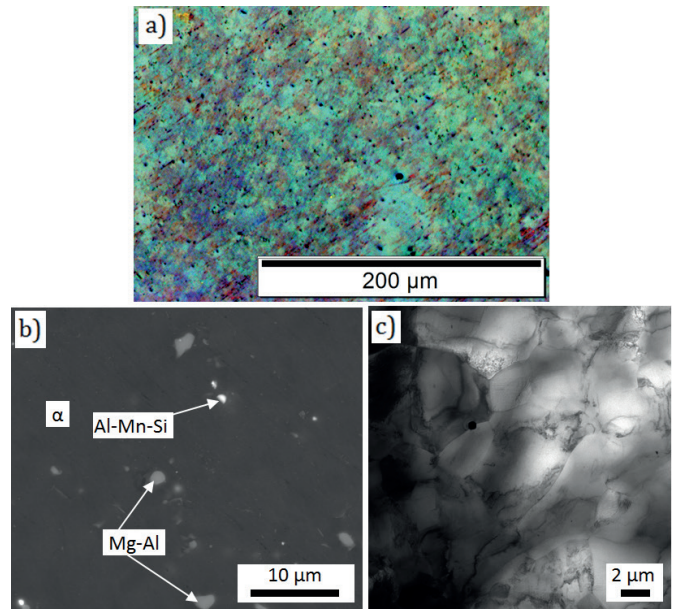
Fig. 1. Microstructure in the cross-section of AZ61-P rod in F condition observed by light microscopy (a), SEM (b) and TEM (c)
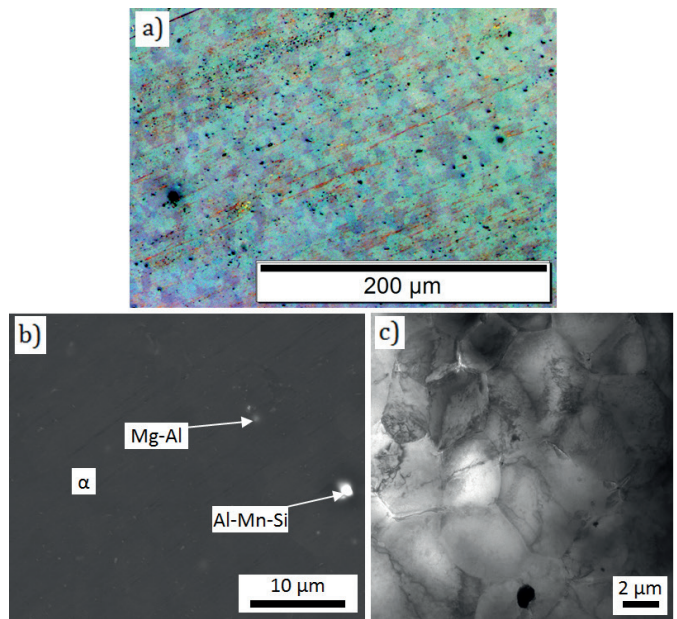
Fig. 2. Microstructure in the cross-section of AZ61-CRE rod in F condition observed by light microscopy (A), SEM (B) and TEM (c)

TABLE 1

The designation of test material and the results of chemical analysis made by optical emission spectrometry

| Material symbol | Method of extrusion | Element [%weight] | | | | | | | |
|---|---|---|---|---|---|---|---|---|---|
| | | Al | Zn | Mn | Cu | Ni | Fe | Si | Mg |
| AZ61-P | Direct extrusion | 6.26 | 0.74 | 0.22 | 0.003 | 0.001 | 0.004 | 0.03 | bal. |
| AZ61-CRE | Continuous rotary extrusion | | | | | | | | |

TABLE 2

Hardness values and average grain size observed in the cross-section of AZ61-P and AZ61-CRE rods in F condition

| Material symbol | Hardness [HBW 2.5/62.5] | Average grain size [μm] |
|---|---|---|
| AZ61-P | 71.3 | 5.5 |
| AZ61-CRE | 69.0 | 7.7 |

As revealed by the texture analysis, in the AZ61-P alloy in F condition (Fig. 3a), the dominant orientations were {100} to {110} with the prevalence of {100}. The material had a fibrous texture typical of extruded magnesium alloys, i.e. the arrangement of magnesium grains wherein the {100} lattice planes are parallel (or almost parallel) to the rod cross-section. The texture of the rod processed by CRE (Fig. 3b) can be considered weak because the degree of texturing does not exceed the level 3. This texture deviates from the typical texture of extruded rods. The predominant orientations are those described with the indices (hk0), situated on the circumference of a circle of the stereographic projection.
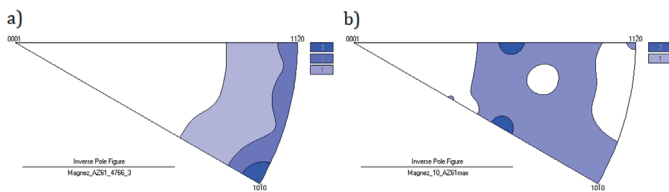


Fig. 3. Inverse pole figures in the cross-section of AZ61-P rod (a) and AZ61-CRE rod (b) in F condition

In the next stage of studies, the test rods were subjected to a two-step heat treatment (solutionizing and aging) with measurement of respective hardness values. Based on the hardness measurements, aging curves were plotted as shown in Figure 4. The highest hardness was observed after 192 hours of aging (T6 condition) for both alloys, i.e. extruded in the direct process (78 HB) and subjected to CRE (74.3 HB). The maximum hardness of profile made by the direct extrusion and subjected to a two-step heat treatment was by 3.7 HB higher than the respective value obtained for CRE rod.
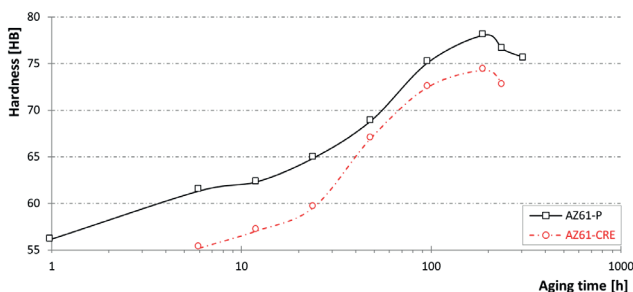


Fig. 4. Hardness of AZ61 and AZ61-P-CRE profiles after solution heat treatment and aging

Figure 5 shows microstructure with revealed grains observed in the AZ61-P and AZ61-CRE alloys after solution heat treatment and aging for 96 h. During high temperature annealing in the process of solution heat treatment, the grain growth was observed to occur. In the case of AZ61-P alloy (Fig. 5a), the average grain size increased from 5.5 μm to 14.8 μm, while for the AZ61-CRE alloy (Fig. 5b), the increase was from 7.7 μm to 20 μm.
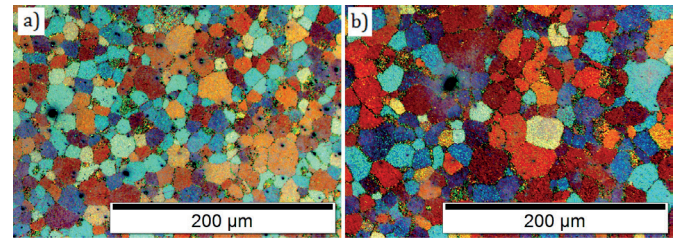


Fig. 5. Microstructure with revealed grains observed in the cross-section of AZ61-P rod (a) and AZ61-CRE rod (b) both solution treated and aged for 96 h

Fine-dispersed phases precipitating during aging of the AZ61-P alloy were identified by electron diffraction (Fig. 6). The presence of $Mg_{17}Al_{12}$ phase with cubic crystallographic lattice and space group I-43m was revealed. The precipitates of this phase were arranged in the [T2T0] direction with respect to α solution.
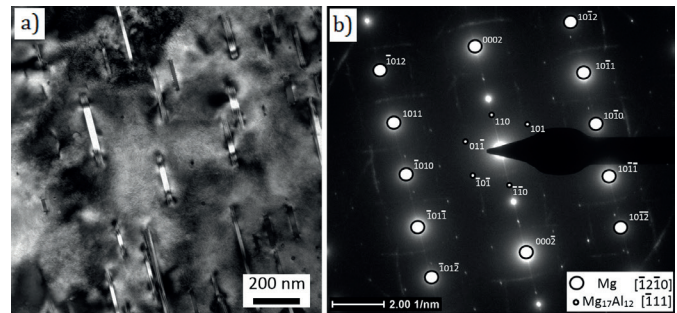


Fig. 6. Dark field TEM image of microstructure (a) obtained for the AZ61-P alloy solution treated and aged for 96 hours and selected area electron diffraction pattern with the solution for β-$Mg_{17}Al_{12}$ phase (b)

Microstructures of the AZ61-P alloy after solution heat treatment and different times of aging are presented in Figures 7 and 8 for the SEM and TEM examinations, respectively.

Detailed examinations showed that after one hour aging the decomposition of solid solution took place with the precipitation of fine-dispersed, spheroidal and lamellar particles of the size from 10 nm up to about 50 nm. After 6 hours of aging, the precipitates appeared at grain boundaries (single plates of the size not exceeding 1 μm) and inside the grains (very dense, fine-dispersed particles). Aging for 96 hours resulted in the growth of plates of the continuous β phase and in the formation of a discontinuous β phase precipitating as a eutectic in the direction from the edge to the centre of grains. Aging for 192 hours, which corresponded to the T6 condition, has increased the density of the fine plates of the continuous β phase. They had the thickness of 35 nm and different lengths. The presence of a particle free zones (PFZ) were also observed. After aging for 312 hours (with hardness decreasing), the growth of the plates of the continuous β phase took place inside the grains. The increase in the thickness of the plates was not uniform, assuming higher values in the grains with larger diameters.
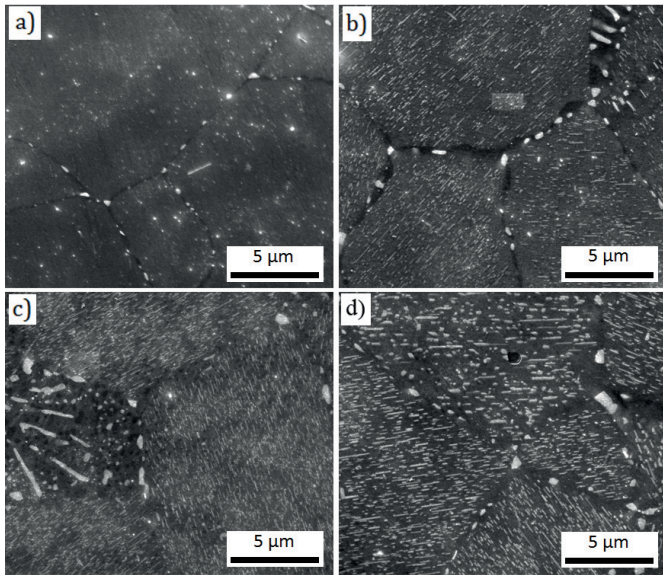
Fig. 7. SEM microstructure in the cross-section of AZ61-P rod solution treated and aged for 6 h (a), 96 h (b), 192 h (c) and 312 h (d)
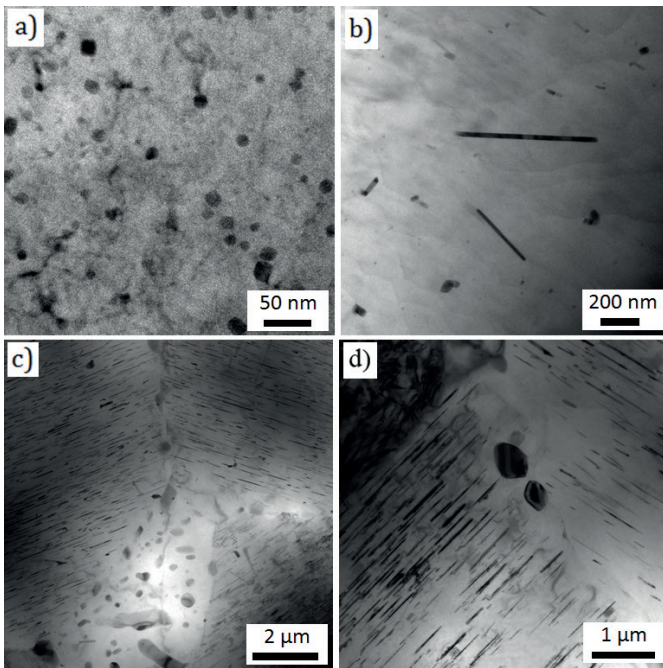


Fig. 8. TEM microstructure in the cross-section of AZ61-P rod solution treated and aged for 1 h (a), 6 h (b), 96 h (c, d)

The SEM and TEM structures of the AZ61-CRE rod solution treated and aged for 96 h are shown in Figures 9 and 10, respectively. The plates of the continuous β phase are not oriented in any preferred direction. In the cross-section, they are intersected in both longitudinal and transverse directions. This proves weak texturing, since the precipitates of β phase are arranged in accordance with the crystallographic direction of individual grains. Numerous large precipitates of the β phase are observed at grain boundaries as compared with the material extruded by direct process.
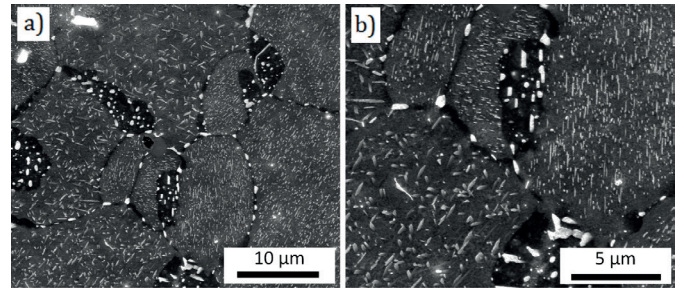


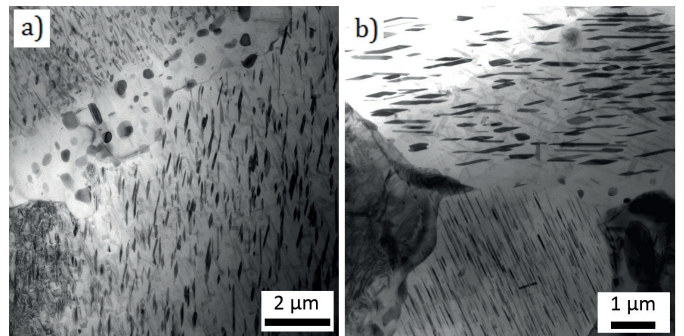Fig. 9. SEM microstructure in the cross-section of AZ61-CRE rod solution treated and aged for 96 h



Fig. 10. TEM microstructure in the cross-section of AZ61-CRE rod solution treated and aged for 96 h

Examinations of the longitudinal section of the AZ61-P alloy (Fig. 11a) solution treated and aged for 96 hours lead to the conclusion that plates of the β phase inside the grains precipitate mainly in direction parallel to the direction of extrusion. In the longitudinal section of AZ61-CRE alloy (Fig. 11b), similar as in the cross-section, the plates of β phase take an arbitrary direction consistent with the grain orientation. The precipitation of $Mg_{17}Al_{12}$ phase along the direction of extrusion proves stronger anisotropy of the AZ61-P alloy as compared to the AZ61-CRE alloy.
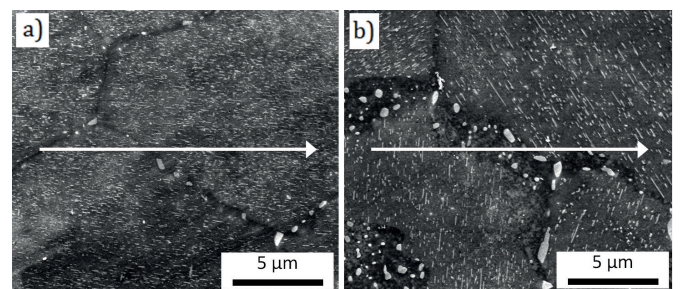


Fig. 11. SEM microstructure in the longitudinal section of AZ61-P rod (a) and AZ61-CRE rod (b) both solution treated and aged for 96 hours with the indicated direction of extrusion

In Table 3 are compared the results of hardness measurements taken in the cross-section and longitudinal section of profiles extruded from the AZ61-P and AZ61-CRE alloys solution treated and aged for 192 h. Treated to this condition, the AZ61-P rod shows significantly different

hardness values in the cross-section (78.1 HB) and longitudinal section (71.6 HB). This demonstrates the anisotropic properties of material extruded by the direct process. Strong texture leads to the anisotropy of mechanical properties in the direction of the texture and reduced yield strength in compression, as compared to tension [7]. The alloy extruded by CRE has weaker texture and lack of anisotropic properties, which translates into the hardness values identical in both sections.

TABLE 3

Longitudinal and transverse hardness of the AZ61 and AZ61-P-CRE profiles solution treated and aged for 192 h

| Section<br>Material symbol | Hardness<br>[HBW 2.5/62.5] | |
|---|---|---|
| | Cross-section | Longitudinal section |
| AZ61-P | 78.1 | 71.6 |
| AZ61-CRE | 74.3 | 74.2 |

## 4. Summary

Based on the results of studies it was found that AZ61 magnesium alloy rods produced by the processes of direct extrusion and continuous rotary extrusion are prone to precipitation hardening. To obtain the T6 condition (maximum hardness), aging for 192 hours is required in the case of used two-step heat treatment. Longer aging results in hardness decrease. Hardness in the cross-section of alloy extruded by direct process is higher compared to the material obtained by CRE.

*Received: 10 March 2015.*

Two-step heat treatment results in the grain growth. This process occurs primarily at the annealing stage of solution heat treatment. Long annealing causes grain growth, which can deteriorate the mechanical properties after aging. Contrary to the alloy processed by CRE, the alloy extruded by direct process is characterized by a strong texture and anisotropy of mechanical properties. During aging, in the solution treated AZ61 alloy, the precipitation of intermetallic $\beta$-$Mg_{17}Al_{12}$ phases takes place. The precipitation of $\beta$ phase is discontinuous at the grain boundaries and continuous in the form of plates in the grain interior. The plates are arranged in a preferred direction relative to the crystallographic orientation of individual grains.

## REFERENCES

[1] R. Senthil, A. Gnanavelbabu, Appl Mech Mater 606, 55-59 (2014), DOI:10.4028/www.scientific.net/AMM.**606**.55.
[2] A. Dziadon, R. Mola, Met Form **24**, 4, 253-277 (2013).
[3] http://www.gbv.de/dms/clausthal/E_DISS/2012/db110731.pdf.
[4] R. Zeng, Precipitation hardening in AZ91 magnesium alloy, PhD thesis, University of Birmingham, Birmingham, B15 2TT, July (2013)
[5] B. Płonka, J. Kut, P. Korczak, M. Lech-Grega, M. Rajda, Arch Metall Mater, **57**, 619-626 (2012), DOI: 10.2478/v10172-012-0066-8.
[6] B. Płonka, K. Remsak, M. Nowak, M. Lech-Grega, P. Korczak, Materials Science Forum, Tchermec 2013, **783-786**, 443-448 (2014), DOI: 10.4028/www.scientific.net/MSF.783-786.443.
[7] T. Reguła, E. Czekaj, A. Fajkiel, M. Lech-Grega, M. Bronicki, Rudy i Metale Nieżelazne **53**, 7, 430-435 (2008).